ADVANCES IN ATMOSPHERIC SCIENCES, VOL. 32, SEPTEMBER 2015, 1255–1265

Synergistic Contribution of Precipitation Anomalies over Northwestern India and the South China Sea to High Temperature over the Yangtze River Valley

LIU Ge*[1], WU Renguang[2,3], SUN Shuqing[4], and WANG Huimei[1]

[1]*Chinese Academy of Meteorological Sciences, Beijing* 100081

[2]*Institute of Space and Earth Information Science/Department of Geography and Resource Management/Shenzhen Research Institute, Chinese University of Hong Kong, Hong Kong SAR*

[3]*Center for Monsoon System Research, Institute of Atmospheric Physics, Chinese Academy of Sciences, Beijing* 100029

[4]*State Key Laboratory of Numerical Modeling for Atmospheric Sciences and Geophysical Fluid Dynamics, Institute of Atmospheric Physics, Chinese Academy of Sciences, Beijing* 100029

(Received 23 December 2014; revised 26 February 2015; accepted 17 March 2015)

ABSTRACT

This study explores the characteristics of high temperature anomalies over eastern China and associated influencing factors using observations and model outputs. Results show that more long-duration (over 8 days) high temperature events occur over the middle and lower reaches of the Yangtze River Valley (YRV) than over the surrounding regions, and control most of the interannual variation of summer mean temperature *in situ*. The synergistic effect of summer precipitation over the South China Sea (SCS) region (18°–27°N, 115°–124°E) and the northwestern India and Arabian Sea (IAS) region (18°–27°N, 60°–80°E) contributes more significantly to the variation of summer YRV temperature, relative to the respective SCS or IAS precipitation anomaly. More precipitation (enhanced condensational heating) over the SCS region strengthens the western Pacific subtropical high (WPSH) and simultaneously weakens the westerly trough over the east coast of Asia, and accordingly results in associated high temperature anomalies over the YRV region through stimulating an East Asia–Pacific (EAP) pattern. More precipitation over the IAS region further adjusts the variations of the WPSH and westerly trough, and eventually reinforces high temperature anomalies over the YRV region. Furthermore, the condensational heating related to more IAS precipitation can adjust upper-tropospheric easterly anomalies over the YRV region by exciting a circumglobal teleconnection, inducing cold horizontal temperature advection and related anomalous descent, which is also conducive to the YRV high temperature anomalies. The reproduction of the above association in the model results indicates that the above results can be explained both statistically and dynamically.

Key words: high temperature events, Yangtze River Valley, precipitation, ECHAM5

Citation: Liu, G., R. G. Wu, S. Q. Sun, and H. M. Wang, 2015: Synergistic contribution of precipitation anomalies over northwestern India and the South China Sea to high temperature over the Yangtze River Valley. *Adv. Atmos. Sci.*, **32**(9), 1255–1265, doi: 10.1007/s00376-015-4280-y.

1. Introduction

High temperature events (heat waves) are one of the most important types of meteorological disaster occurring in summer. High temperature events with long duration substantially affect people's lives and the economy because of the associated increased consumption of water and electricity, and the destructive consequences for agriculture. The number of consecutive days, strength, and frequency of high temperature events in China have shown an increasing trend since the 1990s (Lin and Guan, 2008; Ye et al., 2013). Individual examples include: the persistent high temperature event during the summer of 2002 experienced in northern China (Wei et al., 2004); the high temperature event that covered a broad area of southern China in the summer of 2003 (Wang et al., 2006); the persistent event with extremely high temperature and severe drought that occurred over southwestern China during July–September 2006 (Peng et al., 2007; Li et al., 2011); and the high temperature event over southern China during the summer of 2013 that showed an unprecedented areal extent, duration, and maximum temperature, and which even caused the deaths of many people (Peng, 2014). Therefore, it is important to understand the variability of high temperature anomalies and associated factors and mechanisms.

Numerous case studies have revealed that the western Pa-

* Corresponding author: LIU Ge
Email: liuge@cams.cma.gov.cn

cific subtropical high (WPSH) is an important factor directly causing summer high temperature events over various regions of China (Wei et al., 2004; Wei and Sun, 2007; Peng et al., 2007; Zou and Gao, 2007; Shi et al., 2009; Li et al., 2011; Chen et al., 2013). High temperature events tend to occur over the regions where the WPSH dominates. The strong and stable WPSH, which directly resulted in high temperature over southern China during the summer of 2013, was associated with the anomalies of surrounding circulation systems, such as a stronger South Asian high (SAH), weaker cold air activity from high latitudes, and stronger convection in the tropics (Peng, 2014).

Numerical simulations and theoretical analyses have further revealed the effects of convective heating and SST anomalies over tropical oceans on the formation and variability of the WPSH. Through triggering a meridional quasi-stationary planetary Rossby wave, anomalous convective activity in the western Pacific warm pool results in the East Asia–Pacific (EAP), or Pacific–Japan (PJ), teleconnection pattern and therefore modulates the WPSH (Nitta, 1987; Huang and Li, 1988; Huang and Sun, 1992). The latent heating over the region from India to the Indo-China Peninsula via the Bay of Bengal, which is released by monsoon rainfall, forces the SAH (WPSH) on the western (eastern) side of this heating center (Liu et al., 1999; Liu and Wu, 2004). It has long been known that the WPSH is intensified and shifts southward during El Niño decaying summers (Huang et al., 1996; Wang et al., 2000; Chang et al., 2000). Indian Ocean warming is also an important factor, which explains why the WPSH is abnormally strong in summer after the El Niño anomaly becomes weak (Xie et al., 2009). Tropical Indian Ocean warming can stimulate low-level anomalous anticyclonic circulation over the subtropical northwest Pacific Ocean and southern China (i.e. the WPSH) by emanating a warm Kelvin wave (Hu et al., 2012). Recently, Wang et al. (2013) suggested that variation of the WPSH is primarily controlled by central Pacific cooling/warming and a positive atmosphere–ocean feedback mechanism between the WPSH and the Indo-Pacific warm pool oceans.

The present study analyzes the characteristics of high temperature events over eastern China and investigates the influences of tropical circulation and SST anomalies. The rest of the paper is organized as follows: In section 2, we describe the data. Section 3 presents the temporal and spatial features of high temperature events in summer. The factors of summer temperature anomalies and associated physical processes are also investigated in section 3. The results derived from observations in section 3 are further examined in section 4 based on outputs from the European Centre Hamburg 5/Max Planck Institute-Ocean model (ECHAM5/MPI-OM). Finally, a summary and discussion are provided in section 5.

2. Data

The Asian Precipitation Highly Resolved Observational Data Integration towards the Evaluation of Water Resources (APHRODITE) surface air temperature (SAT) dataset is used in the present study. This is a daily temperature dataset on grids of $0.5^\circ \times 0.5^\circ$ covering the Asian monsoon region (15°S–55°N, 60°–150°E) (Yasutomi et al., 2011). The other temperature dataset used in this study is the monthly mean temperature at 160 stations from the National Climate Center, China. The present study also uses monthly mean geopotential height from the National Centers for Environmental Prediction (NCEP)–Department of Energy (DOE) Reanalysis 2 (Kanamitsu et al., 2002), the Climate Prediction Center (CPC) Merged Analysis of Precipitation (CMAP; Xie and Arkin, 1997), the National Oceanic and Atmospheric Administration (NOAA) interpolated outgoing long wave radiation (OLR; Liebmann and Smith, 1996), and the NOAA extended reconstructed version 3b SST (Smith et al., 2008). The above datasets are all available from 1979 to 2007.

In addition, the ECHAM5/MPI-OM outputs (monthly mean SAT and precipitation) prepared for the Intergovernmental Panel on Climate Change (IPCC) Fourth Assessment Report's Climate of the 20th Century Experiment (20C3M) (Jungclaus et al., 2006), which are available on 192×96 longitude-latitude Gaussian grids, are used to verify the observed results.

3. High temperature events and associated factors

3.1. *The characteristics of high temperature events over eastern China*

In the present study, daily mean SAT with an anomaly over 1°C is referred to as high temperature. The duration of high temperature events is defined as the number of consecutive days with high temperature. A high temperature event is considered as a summer event if the central day of the event (or the prior day if the event persists for an even number of days) falls in the period from 1 June to 31 August.

High temperature events with longer duration have larger influences than those with shorter duration. Figure 1 presents climatological mean numbers of summer high temperature events with long duration (over 8 days) over eastern China. As shown in Fig. 1, high temperature events with duration over 8 days cover two regions of large number, one over the mid–high latitudes to the north of 40°N, and the other over the middle and lower reaches of the Yangtze River Valley (YRV). In this study, we primarily explore the latter since the middle and lower reaches of the YRV is a crucial region for agriculture, and features relatively more long-duration (over 8 days) high temperature events than the surrounding regions (Fig. 1).

The number of over-8-day high temperature events averaged over the middle and lower reaches of the YRV (27°–33°N, 111°–123°E) shows significant positive correlation with summer (June–July–August) mean temperature *in situ*, with a coefficient of correlation center of over 0.7 (Fig. 2a). Meanwhile, area-mean summer temperature over the same region has a consistent increasing trend and interannual variation with the area-mean number of over-8-day events

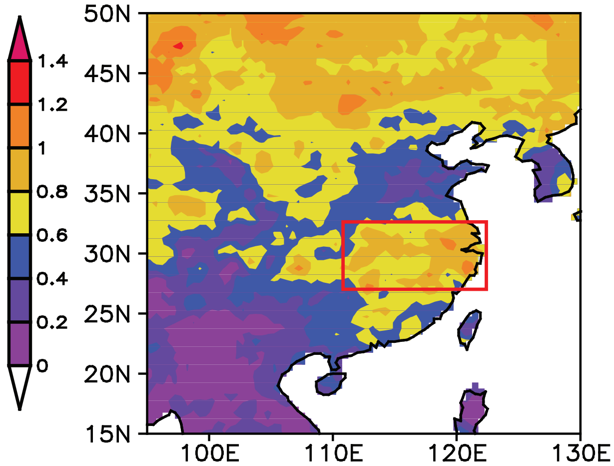

Fig. 1. Climatological mean (1979–2007) number of summer high temperature events (daily temperature mean anomaly higher than 1°C) spanning over eight consecutive days.

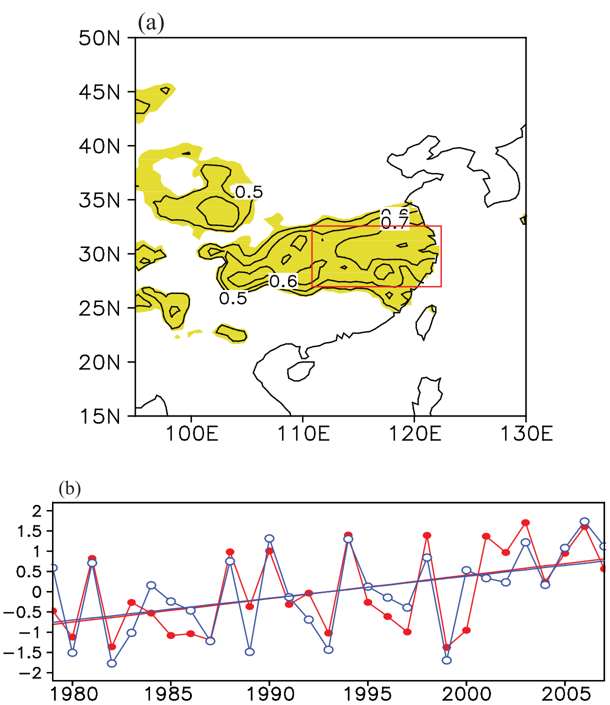

Fig. 2. (a) Distribution of the coefficients of correlation between the number of summer long-duration high temperature events averaged over the middle and lower reaches of the YRV (27°–33°N, 111°–123°E; red box) and summer mean temperature during 1979–2007. Shading denotes that the correlation is significant at the 99% confidence level. (b) Normalized time series of the number of high temperature events (red line) and summer mean temperature (blue line) over the YRV region and their linear trends (red for the former, and blue for the latter).

(Fig. 2b). The correlation coefficient between the two original (detrended) time series is 0.81 (0.75) for the period 1979–2007. Additionally, the mean summer temperature of 23 stations within the YRV region is highly consistent with the number of over-8-day events, with a correlation coefficient of 0.78 (0.72) between the two original (detrended) time series. This further confirms the close relationship between the number of over-8-day events and summer mean temperature.

Furthermore, the number of short-duration (3–8 days) high temperature events averaged over the YRV region is calculated, and is found to be also significantly correlated with summer mean temperature in situ, but with a relatively lower correlation coefficient of 0.71 (0.57) between the two original (detrended) time series. The results reveal that the variation of summer mean temperature over the YRV region can be more attributed to long-duration (over 8 days) high temperature events than to short-duration (3–8 days) events.

Referring to the definition of high temperature events presented by Lau and Nath (2014), a 3–8-day (over-8-day) high temperature event is identified in the YRV region when the spatial mean SAT is higher than the 70th percentile values of this population of daily mean SATs for 3–8 (over 8) consecutive days. Based on this definition, the number of over-8-day events is also significantly correlated with summer mean temperature, with a correlation coefficient of 0.54 (0.51) between the two original (detrended) time series. The relationship between the number of 3–8-day events and summer mean temperature is relatively weaker, with a correlation coefficient of 0.38 (0.34) between the two original (detrended) time series. This further supports the notion that the variation of summer temperature over the YRV region tends to be modulated more by long-duration events than by short-duration events. Therefore, we pay more attention to long-duration (over 8 days) events in this study.

High temperature events with short duration are related to various individual weather systems and are largely due to internal atmospheric processes, while high temperature events with long duration are likely connected to persistent large-scale circulation systems and sustainable external forcing. As such, it is easier to identify the influencing factors of summer temperature and associated mechanisms over the YRV region where long-duration high temperature events control the variation of summer mean temperature. For convenience, the summer mean temperature averaged over the YRV region is defined as the YRV temperature index, which also reflects the variation in the number of long-duration (over 8 days) high temperature events because of their consistency.

3.2. *Factors affecting summer temperature over the YRV region*

The correlation between the summer YRV temperature index and simultaneous 500 hPa geopotential height during 1979–2007 displays a significant positive correlation over the Yellow Sea and the Yangtze and Hwai River Valley region (Fig. 3a), which indicates that, corresponding to the positive geopotential height anomaly over this region, summer high temperature anomalies appear over the YRV region. This positive geopotential height anomaly reflects the fact that the westerly trough is weaker over the east coast of Asia and the WPSH is stronger and extends much farther west and north than normal. A weaker westerly trough implies a weaker intrusion of cold air from the high latitudes, and

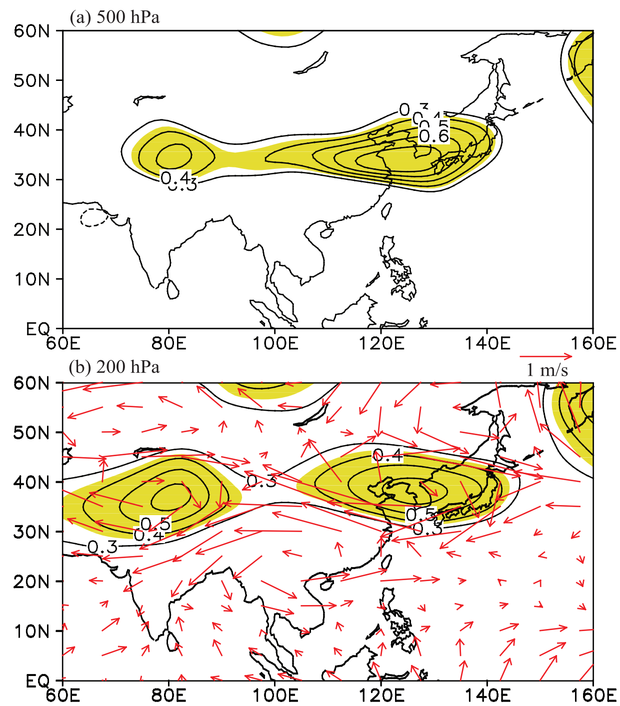

Fig. 3. Distribution of the coefficients of correlation between the summer YRV temperature index and simultaneous (a) 500 hPa and (b) 200 hPa geopotential height (contours) during 1979–2007; red vectors in (b) indicate the anomalous 200 hPa winds regressed by the summer YRV temperature index. Shading denotes that the correlation is significant at the 95% confidence level.

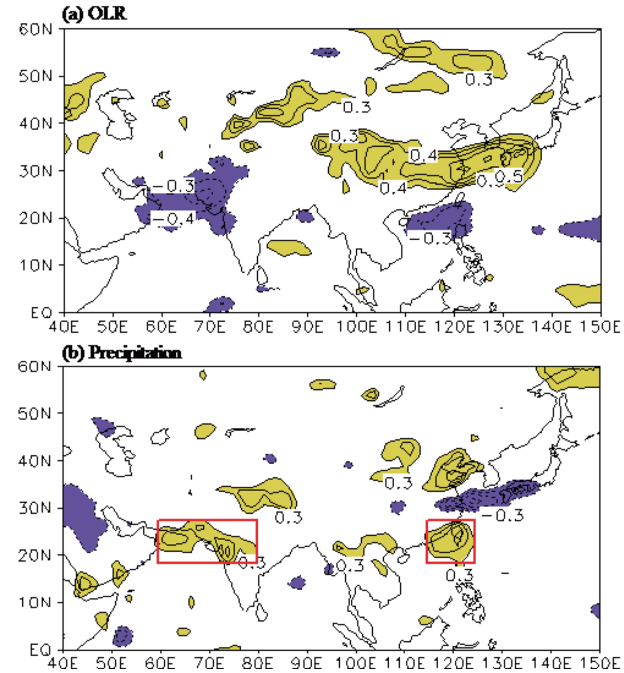

Fig. 4. (a) Distribution of the coefficients of correlation between the summer YRV temperature index and simultaneous OLR during 1979–2007; (b) as in (a) but for the correlation between the YRV temperature index and precipitation, and red boxes denote the IAS (18°–27°N, 60°–80°E) and SCS (18°–27°N, 115°–124°E) regions. Shading denotes that the correlation is significant at the 90% confidence level.

the westward/northward-extended WPSH can directly control eastern China and therefore result in less precipitation and more solar radiation reaching the Earth's surface, which are both conducive to high temperature anomalies over the YRV region.

The correlation between the summer YRV temperature index and simultaneous 200 hPa geopotential height (Fig. 3b) shows a significant positive correlation from North China via the Korean Peninsula to southern Japan. Accompanying this positive geopotential height anomaly and associated anomalous anticyclone, upper-level easterly anomalies prevail over the YRV region, which can induce cold horizontal temperature advection from colder oceanic regions to warm continental Asia and consequently result in anomalous descent and associated high temperature anomalies over the YRV region through adiabatic warming (Hu et al., 2013).

The correlation between the summer YRV temperature index and simultaneous OLR during 1979–2007 (Fig. 4a) shows a significant positive correlation over the YRV region. Correspondingly, a significantly negative correlation exists *in situ* between the summer YRV temperature index and simultaneous precipitation (Fig. 4b). That is, the high temperature anomalies over the YRV region are intimately linked with less local precipitation. High temperature and drought tend to occur concurrently.

Furthermore, it can be seen in Fig. 4a that there are significant negative correlations over two regions: one being the Arabian Sea and northwestern India, and the other the northern part of the South China Sea. Consistently, there are significant positive correlations between the summer YRV temperature index and simultaneous precipitation in these two regions (Fig. 4b). The above correlations remain after removing the linear trends (figure not shown). This implies that, on the interannual scale, corresponding to stronger convection activity and more precipitation over the Arabian Sea and northwestern India and the South China Sea, summer temperature over the YRV region is relatively higher.

Stronger convective activity and more precipitation signify enhanced condensational heating. The condensational heating released by precipitation over different regions can modulate the WPSH in different ways (Nitta, 1987; Huang and Li, 1988; Huang and Sun, 1992; Liu et al., 1999; Liu and Wu, 2004). To investigate the effects of precipitation (condensational heating) over different regions on the WPSH, summer precipitation averaged over the South China Sea region (18°–27°N, 115°–124°E) and over the northwestern India and Arabian Sea region (18°–27°N, 60°–80°E) are referred to as the summer SCS and IAS precipitation indices, respectively. The correlation coefficient between the SCS and IAS precipitation indices is −0.08, revealing that precipitation variations over the two regions are independent from each other. Summer precipitation averaged over both the SCS and IAS regions is defined as the SCS–IAS precipitation index, to reflect the synthesized variation of precipitation (condensational heating) over the two regions.

The correlation between the SCS precipitation index and 500 hPa geopotential height (Fig. 5a) shows a clear negative–positive–negative pattern along the east coast of Asia, with a significant positive correlation from the Bohai Sea to Japan via the Korean Peninsula. The negative–positive–negative pattern is clearly related to the EAP/PJ teleconnection. This implies that the SCS precipitation anomaly may affect the WPSH through stimulating the meridional quasi-stationary planetary Rossby wave from the tropics to the high latitudes.

As for the effect of the IAS precipitation anomaly, the correlation between the IAS precipitation index and geopotential heights displays significant positive correlations along 30°N from 80°E to 130°E, to the northeast of the IAS precipitation anomaly at the 500 hPa level (Fig. 5c), and significant positive correlations over west-central Asia centered on (35°N, 60°E), to the northwest of the IAS precipitation at the 200 hPa level (Fig. 5d). That is, more precipitation (condensational heating) over the IAS region corresponds to positive geopotential anomalies over its western side in the upper troposphere and over its eastern side in the middle troposphere, which is generally consistent with atmospheric responses at different levels to convective condensational heating (Liu et al., 1999, Fig. 2c). This supports the notion that the effect of the vertical gradient of strong condensational heating, which is directly related to the IAS precipitation, plays an important role in modulating the WPSH and the upper-tropospheric geopotential height anomaly over west-central Asia.

In addition to the significant positive correlation over west-central Asia, we can also detect a significant positive correlation from North China to the Korean Peninsula in the upper troposphere (Fig. 5d). The upper-tropospheric pattern with the two anomalies over west-central Asia and East Asia constitutes the Asian part of the circumglobal teleconnection identified by Ding and Wang (2005). This pattern has been indicated to play an important role in connecting the Indian

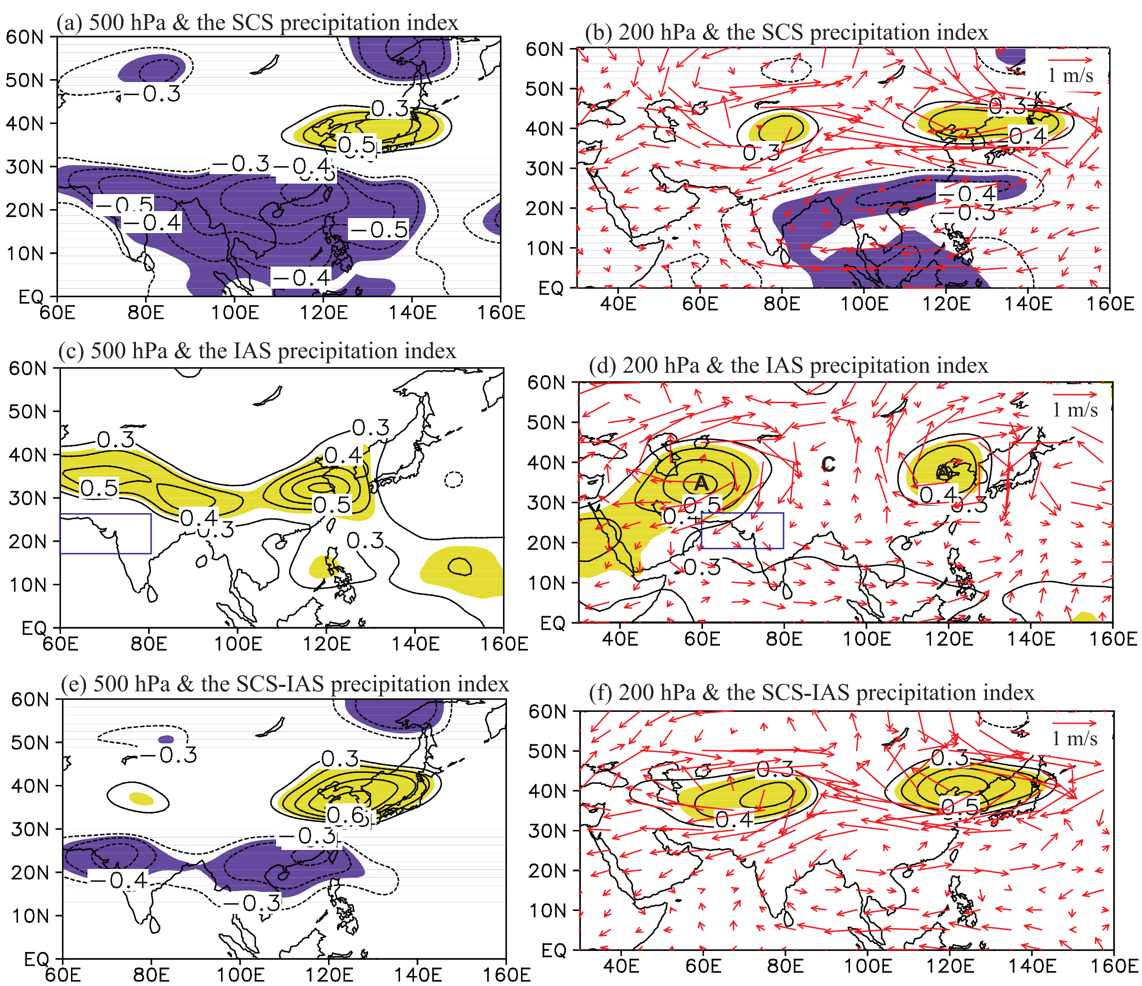

Fig. 5. Correlations of summer 500 hPa geopotential heights (contours) correlated with the summer (a) SCS, (b) IAS, and (c) SCS–IAS precipitation indices; (b), (d), and (f) indicate 200 hPa geopotential heights (contours) correlated with, and the anomalous 200 hPa winds (red vectors) regressed by, the summer SCS, IAS, and SCS–IAS precipitation indices, respectively. Shading denotes that the correlation is significant at the 95% confidence level. Blue boxes in (c) and (d) represent the IAS region. "C" and "A" in (d) represent the anomalous cyclone and anticyclone, respectively.

and North China summer rainfall variations (Wu, 2002; Wu et al., 2003). The diabatic heating effect of Indian monsoon precipitation may excite an anomalous west-central Asian high and downstream Rossby wave train extending to East Asia, and even to the North Pacific and North America (Ding and Wang, 2005). This mechanism further confirms that the IAS precipitation may stimulate upper-tropospheric geopotential height anomalies over west-central Asia and over East Asia.

Relative to the YRV temperature-related circulation anomalies (Fig. 3), the 500 hPa positive geopotential height anomaly over East Asia, related to more SCS precipitation, is weaker and its southern ridge is farther north (Fig. 5a), while that related to more IAS precipitation is farther south (Fig. 5c). In contrast, this positive geopotential height anomaly at the 500 hPa level, which is remarkably linked with more SCS–IAS precipitation (Fig. 5e), is more consistent with Fig. 3a. Similarly, the positive 200 hPa geopotential height anomaly over East Asia resulting from more SCS–IAS precipitation (Fig. 5f), is also more consistent with Fig. 3b than the SCS-related (Fig. 5b) or IAS-related (Fig. 5d) anomaly. In summary, the synergistic effect of SCS and IAS precipitation plays a more important role in modulating the YRV temperature-related circulation anomalies than the individual effect of SCS or IAS precipitation.

Note that the circulation anomalies forced by the SCS–IAS precipitation anomaly is not a simple superposition of the circulation anomalies stimulated by individual SCS and IAS precipitation anomalies, respectively. This implies that the synergistic contributions of the SCS and IAS precipitation anomalies seem to be nonlinear. The IAS precipitation should be considered as a crucial factor in modulating and reinforcing the circulation anomalies forced by the SCS precipitation; therefore, the synergistic effect of the SCS and IAS precipitation anomalies may exert a more significant influence on summer temperature over the YRV region than the individual effect of the SCS or IAS precipitation anomaly, which can be demonstrated by the correlations of summer temperature with different precipitation indices (Fig. 6).

The correlations show that summer temperature over the YRV region is significantly related to the SCS–IAS precipitation (Fig. 6c), while the individual SCS precipitation affects summer temperature over a farther north and smaller region (Fig. 6a). Similarly, compared to the synergistic effect of the SCS–IAS precipitation (Fig. 6c), the effect of individual IAS on summer temperature over the YRV region is remarkably weaker (Fig. 6b).

Comparing the time series of the summer temperature and precipitation indices (Fig. 7) shows that the variation of summer YRV temperature is significantly related to the variations of SCS and IAS precipitation, with correlation coefficients of 0.50 and 0.44, respectively. Furthermore, the variation of summer YRV temperature has a better relationship with the SCS–IAS precipitation index (Fig. 7c), with a correlation coefficient of 0.68 (significant at the confidence level of 99.9%). After removing the linear trends in these time series, the correlation coefficient of the YRV temperature index with the SCS–IAS precipitation index still reaches 0.66 (significant at the confidence level of 99.9%), which is remarkably higher than the correlation coefficient with the individual SCS or IAS precipitation index (both 0.46). In other words, the interannual variation of summer temperature over the YRV region is mainly due to the synergistic effect of summer precipitation

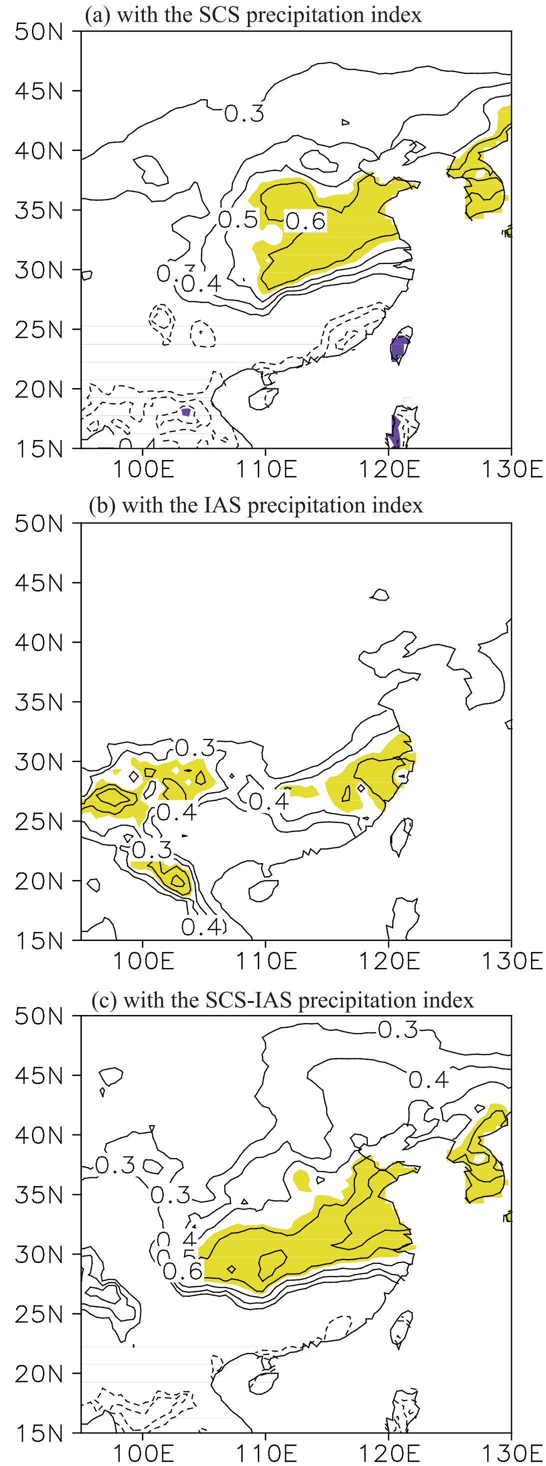

Fig. 6. Distributions of the correlation coefficients of summer temperature with the (a) summer SCS precipitation index, (b) summer IAS precipitation index, and (c) summer SCS–IAS precipitation index during 1979–2007. Shading denotes that the correlation is significant at the 99% confidence level.

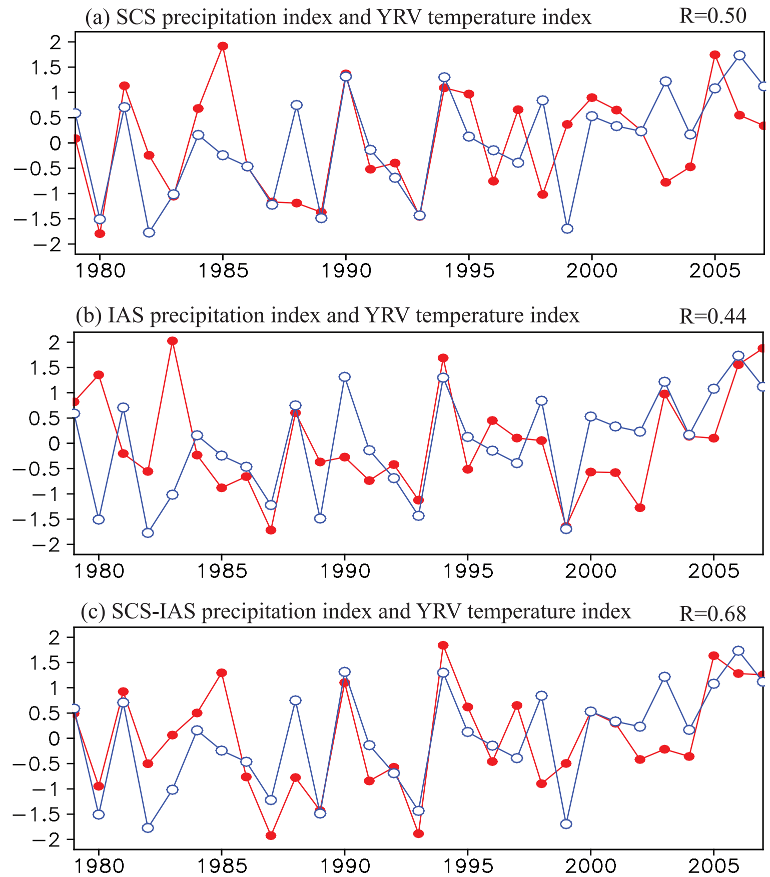

Fig. 7. (a) Normalized time series of the summer SCS precipitation (red line) and YRV temperature (blue line) indices; (b) and (c) as in (a), but for the IAS precipitation index (red line) and the SCS–IAS precipitation index (red line), respectively.

(condensational heating) over the SCS and IAS regions.

4. Results in ECHAM5

To further reveal the relationship between the summer YRV temperature and tropical precipitation (condensation heating), we examine the above results using ECHAM5/MPI-OM model outputs (20c3m). In ECHAM5, the same YRV region (27°–33°N, 111°–123°E) is chosen to define the summer YRV temperature index. Figure 8 presents the correlation between the summer YRV temperature index and simultaneous precipitation during 1979–2007 in ECHAM5. As shown in Fig. 8, there are significant positive correlations over the SCS region and the northwestern India and Arabian Sea region, resembling the correlations in observation (Fig. 4b).

Based on the locations of positive correlations in ECHAM5 (red boxes in Fig. 8), summer precipitation averaged over the SCS region (17°–23°N, 112°–120°E) and over the northwestern India and Arabian Sea region (13°–23°N, 65°–78°E) are defined as the summer SCS and IAS precipitation indices, respectively, and summer precipitation averaged over the above SCS and IAS regions is referred to as the SCS–IAS precipitation index. The correlations of summer temperature with the summer SCS and IAS precipitation indices (Figs. 9a and b) display a significant positive correlation over the YRV region. This signifies that the anomalies of summer SCS and IAS precipitation respectively contribute, to some extent, to the variation of summer temperature over the YRV region. The correlation between the summer SCS–IAS precipitation index and simultaneous temperature (Fig. 9c) shows more significant positive correlations, with two centers over the upper reaches of the YRV and over the middle and

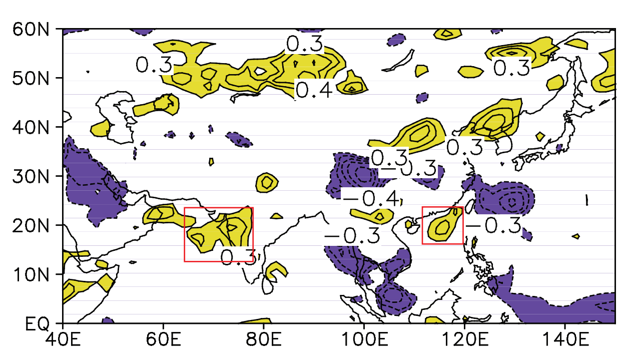

Fig. 8. As in Fig. 4b, but for ECHAM5.

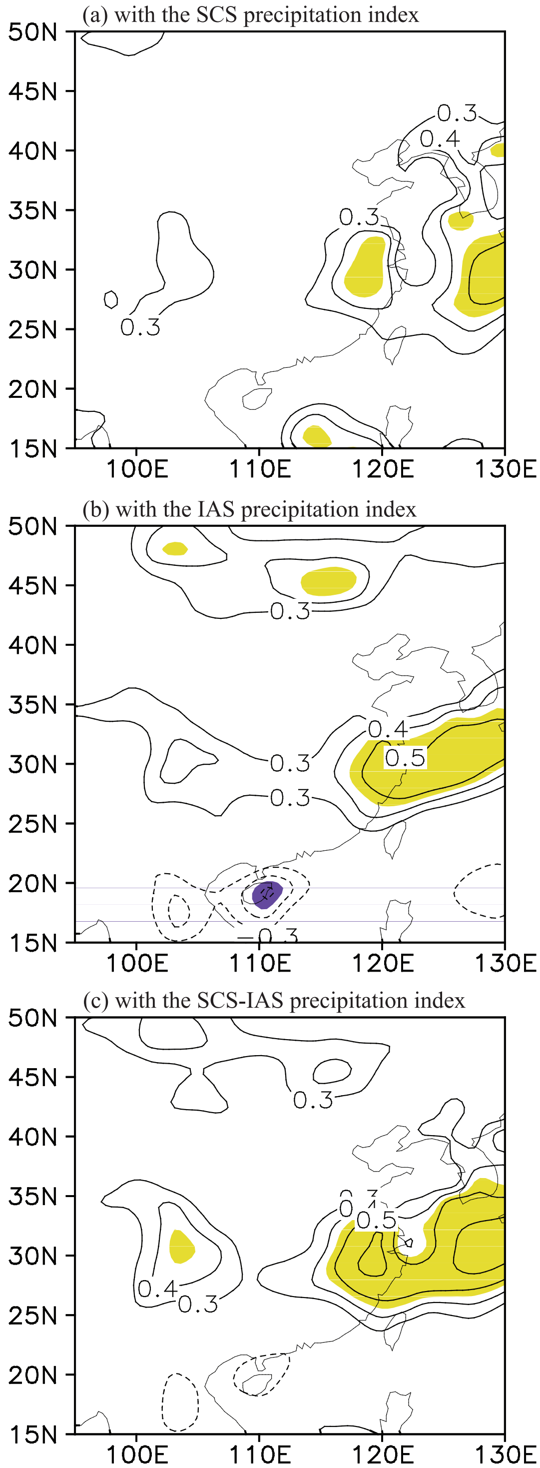

Fig. 9. As in Fig. 6, but for ECHAM5.

lower reaches of the YRV. The result is more similar to the observed summer temperature anomalies resulting from high temperature events (Fig. 2a), which verifies the synergistic effect of the SCS–IAS precipitation in modulating summer temperature over the YRV region.

Comparing among the time series of these indices (figure not shown) further confirms that, relative to the respective effects of the SCS and IAS precipitation, the synergistic effect of the SCS–IAS precipitation provides a greater contribution to the variation of the YRV temperature. The correlation coefficient of the YRV temperature index with the SCS–IAS precipitation index is 0.50 (significant at the confidence level of 99%), higher than the correlation coefficients with the SCS and IAS precipitation indices (0.37 and 0.46, respectively). After removing the linear trends in these time series, the correlation coefficient of the YRV temperature index with the SCS–IAS precipitation index is 0.51, which is also higher than the correlation coefficients with the individual SCS and IAS precipitation indices (0.40 and 0.45, respectively).

In summary, ECHAM5 captures the relationships between the summer YRV temperature and tropical precipitation over different regions, and confirms that the synergistic contribution of the SCS–IAS precipitation to the summer YRV temperature is stronger than the individual contribution of the SCS or IAS precipitation. This implies that the above results can be explained both statistically and dynamically.

5. Summary and discussion

Using observations and ECHAM5/MPI-OM model outputs prepared for the IPCC Fourth Assessment Report's Climate of the 20th Century Experiment, we investigate the characteristics of high temperature anomalies over eastern China and associated influencing factors. It is found that the middle and lower reaches of the YRV constitute one of the most important regions where more long-duration (over 8 days) high temperature events occur and contribute to a large part of the variation of local summer mean temperature.

The high temperature anomalies over the YRV region are closely related to more precipitation over the SCS and IAS regions. The positive anomaly of precipitation over the SCS region, which corresponds to enhanced condensational heating, stimulates the meridional quasi-stationary planetary Rossby wave from the tropics to the high latitudes along the east coast of Asia and modulates the EAP-like pattern, consequently leading to a weak westerly trough and the westward and northward expansion of the WPSH. Under the abnormal background, more precipitation over the IAS region enhances condensational heating in situ. On the one hand, the strong condensational heating forces a significant positive correlation band in the midlatitudes of Asia, which further results in a weaker westerly trough and a stronger and larger anomaly of the WPSH, eventually increasing summer temperature over the YRV region. On the other hand, this heating excites a circumglobal teleconnection, with a positive geopotential height anomaly over west-central Asia and over downstream East Asia in the upper troposphere. Accompanying this geopotential height anomaly over East Asia and the associated anomalous anticyclone, upper-level easterly anomalies appear over the YRV region and induce cold horizontal temperature advection and related anomalous descent, further leading to high temperature anomalies through adiabatic warming. Through the above processes, the synergistic contribution of the SCS–IAS precipitation to the summer YRV temperature is more significant than the individual

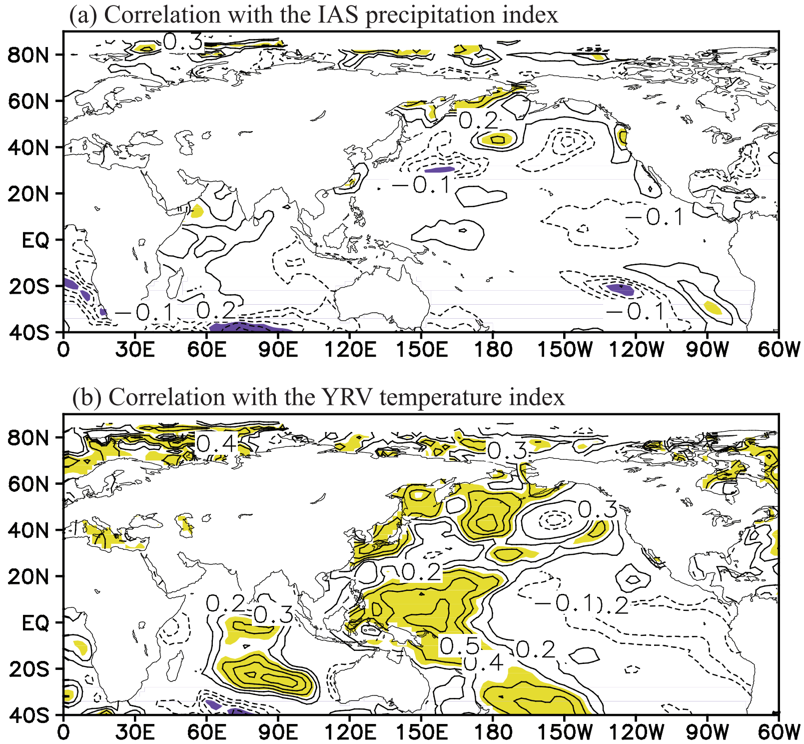

Fig. 10. Distributions of the correlation coefficients of summer SSTs with the (a) summer IAS precipitation index and (b) summer YRV temperature index during 1979–2007. Shading denotes that the correlation is significant at the 95% confidence level.

contribution of the SCS or IAS precipitation. ECHAM5 reproduces and verifies the above results.

Tropical SST anomalies can modulate the variation of the WPSH/SAH (Huang et al., 1996; Wang et al., 2000; Chang et al., 2000; Ding and Wang, 2005; Xie et al., 2009; Huang et al., 2011; Wang et al., 2013) and Indian monsoon precipitation (e.g., Kershaw, 1988; Yang and Lau, 1998; Vecchi and Harrison, 2004). However, the correlation between the summer IAS precipitation index and simultaneous SST indicates that there is no large-range significant relationship between summer IAS precipitation and SSTs (Fig. 10a), while the correlation between the summer YRV temperature index and simultaneous SSTs shows significant positive correlations in the eastern Indian Ocean and the western Pacific warm pool and adjacent seas of East Asia (Fig. 10b). The relationship of SSTs with summer IAS precipitation and that with summer YRV temperature are evidently different from each other (Fig. 10). This inconsistency implies that the concurrent occurrence of more precipitation over the IAS region and high temperature anomalies over the YRV region is not due to simultaneous forcing of SST anomalies. Instead, the IAS precipitation, together with the SCS precipitation, plays an important role in modulating high temperature events and related summer temperature over the YRV region. Wang et al. (2013) demonstrated that a dipolar SST anomaly in the Indo-Pacific warm pool and a significant cooling/warming over the equatorial central-eastern Pacific can control the variation of the WPSH. Nevertheless, the correlation between the summer YRV temperature index and simultaneous SSTs does not show the above features of SST anomalies. This implies that this type of anomalous WPSH, which is a main factor for high YRV temperature, may be adjusted by different external forcing and mechanisms, which is worthy of further investigation.

This study suggests a synergistic contribution of the SCS–IAS precipitation to high temperature events and associated summer temperature over the YRV region. Therefore, to predict high temperature anomalies over the YRV region, we cannot merely focus on the preceding factors of the YRV temperature itself. Exploring the preceding factors of summer precipitation over the SCS and IAS regions is obviously helpful. The Asian climate is related to SST and snow cover and sea ice (Douville and Royer, 1996; Yang and Lau, 1998; Wu and Kirtman, 2007; He et al., 2007; Li et al., 2008; Wu et al., 2009; Wang et al., 2012; Fu and Li, 2013), and thus the potential effects of prior SST, sea ice, and snow cover on summer precipitation over the SCS and IAS regions and related high temperature anomalies over the YRV region should be addressed in the future.

Acknowledgements. The authors wish to thank Dr. PENG Jingbei for her helpful discussion, and the two anonymous reviewers for their useful comments. GL acknowledges the support of the National Natural Science Foundation of China (Grant Nos. 41375090 and 41375091) and the Basic Research Fund of the Chinese Academy of Meteorological Sciences (Grant Nos. 2013Z002 and 2015Z001). RW acknowledges the support of a Direct Grant of the Chinese University of Hong Kong (Grant No. 4052057). We thank the Research Institute for Humanity and Nature (RIHN) for providing the APHRODITE gridded daily temperature dataset through its website (www.chikyu.ac.jp/precip/index.html).

REFERENCES

Chang, C.-P., Y. Zhang, and T. Li, 2000: Interannual and interdecadal variation of East Asian summer monsoon and the tropical Pacific SSTs. Part I: Roles of the subtropical ridge. *J. Climate*, **13**, 4310–4325.

Chen, M., F.-H. Geng, L.-M. Ma, W.-D. Zhou, H. Shi, and J.-H. Ma, 2013: Analyses on the heat wave events in Shanghai in recent 138 years. *Plateau Meteorology*, **32**, 597–607. (in Chinese)

Ding, Q. H., and B. Wang, 2005: Circumglobal teleconnection in the Northern Hemisphere summer. *J. Climate*, **18**, 3483–3505.

Douville, H., and J.-F. Royer, 1996: Sensitivity of the Asian summer monsoon to an anomalous Eurasian snow cover within the Météo-France GCM. *Climate Dyn*., **12**, 449–466.

Fu, J.-J, and S.-L Li, 2013: The influence of regional SSTs on the interdecadal shift of the East Asian summer monsoon. *Adv. Atmos. Sci.*, **30**, 330–340, doi: 10.1007/s00376-012-2062-3.

He, J.-H., J.-H. Ju, Z.-P. Wen, J.-M. Lü, and Q.-H. Jin, 2007: A review of recent advances in research on Asian monsoon in China. *Adv. Atmos. Sci.*, **24**, 972–992, doi: 10.1007/s00376-007-0972-2.

Hu, K. M., G. Huang, X. Qu, and R. H. Huang, 2012: The impact of Indian Ocean variability on high temperature extremes across the southern Yangtze River Valley in late summer. *Adv. Atmos. Sci.*, **29**, 91–100, doi: 10.1007/s00376-011-0209-2.

Hu, K. M., G. Huang, and R. G. Wu, 2013: A strengthened influence of ENSO on August high temperature extremes over the southern Yangtze River valley since the late 1980s. *J. Climate*, **26**, 2205–2221.

Huang, G., X. Qu, and K.-M. Hu, 2011: The impact of the tropical Indian Ocean on South Asian high in boreal summer. *Adv. Atmos. Sci.*, **28**, 421–432, doi: 10.1007/s00376-010-9224-y.

Huang, R.-H., and W.-J. Li, 1988: Influence of heat source anomaly over the western tropical Pacific on the subtropical high over East Asia and its physical mechanism. *Chinese J. Atmos. Sci.*, **12**, 107–116. (in Chinese)

Huang, R.-H., and F.-Y. Sun, 1992: Impacts of the tropical western Pacific on the East Asian summer monsoon. *J. Meteor. Soc. Japan*, **70**, 243–256.

Huang, R.-H., Y.-F. Fu, and X.-Y. Zang, 1996: Asian monsoon and ENSO cycle interaction. *Climate and Environmental Research*, **1**, 38–54. (in Chinese)

Jungclaus, J. H., and Coauthors, 2006: Ocean circulation and tropical variability in the coupled model ECHAM5/MPI-OM. *J. Climate*, **19**, 3952–3972.

Kanamitsu, M., W. Ebisuzaki, J. Woollen, S.-K. Yang, J. J. Hnilo, M. Fiorino, and G. L. Potter, 2002: NCEP–DOE AMIP-II Reanalysis (R-2). *Bull. Amer. Meteor. Soc.*, **83**, 1631–1643.

Kershaw, R., 1988: The effect of a sea surface temperature anomaly on a prediction of the onset of the south-west monsoon over India. *Quart. J. Roy. Meteor. Soc.*, **114**, 325–345.

Lau, N.-C., and M. J. Nath, 2014: Model simulation and projection of European heat waves in present-day and future climates. *J. Climate*, **27**, 3713–3730.

Li, S.-L., J. Lu, G. Huang, and K.-M. Hu, 2008: Tropical Indian Ocean basin warming and East Asian summer monsoon: A multiple AGCM study. *J. Climate*, **21**, 6080–6088.

Li, Y.-H., H.-M. Xu, and D. Liu, 2011: Features of the extremely severe drought in the east of Southwest China and anomalies of atmospheric circulation in summer 2006. *Acta Meteorologica Sinica*, **25**, 176–187.

Liebmann, B., and C. A. Smith, 1996: Description of a complete (interpolated) outgoing longwave radiation dataset. *Bull. Amer. Meteor. Soc.*, **77**, 1275–1277.

Lin, X., and Z.-Y. Guan, 2008: Temporal-spatial characters and interannual variations of summer high temperature in East China. *Journal of Nanjing Institute of Meteorology*, **31**, 1–9. (in Chinese)

Liu, Y.-M., G.-X. Wu, H. Liu, and P. Liu, 1999: The effect of spatially non-uniform heating on the formation and variation of subtropical high. Part III: Condensation heating and South Asia high and western Pacific subtropical high. *Acta Meteorologica Sinica*, **57**, 525–538. (in Chinese)

Liu, Y.-M., and G.-X. Wu, 2004: Progress in the study on the formation of the summertime subtropical anticyclone. *Adv. Atmos. Sci.*, **21**, 322–342, doi: 10.1007/BF02915562.

Nitta, T., 1987: Convective activities in the tropical western Pacific and their impact on the Northern Hemisphere summer circulation. *J. Meteor. Soc. Japan*, **65**, 373–390.

Peng, J.-B., 2014: An investigation of the formation of the heat wave in southern China in summer 2013 and the relevant abnormal subtropical high activities. *Atmos. Oceanic Sci. Lett.*, **7**, 286–290.

Peng, J.-B., Q.-Y. Zhang, and C. Bueh, 2007: On the characteristics and possible causes of a severe drought and heat wave in the Sichuan-Chongqing region in 2006. *Climatic and Environmental Research*, **12**, 464–474. (in Chinese)

Shi, J., Y.-H. Ding, and L.-M. Cui, 2009: Climatic characteristics of extreme maximum temperature in East China and its causes. *Chinese J. Atmos. Sci.*, **33**, 347–358. (in Chinese)

Smith, T. M., R. W. Reynolds, T. C. Peterson, and J. Lawrimore, 2008: Improvements to NOAA's historical merged land-ocean surface temperature analysis (1880–2006). *J. Climate*, **21**, 2283–2295.

Vecchi, G. A., and D. E. Harrison, 2004: Interannual Indian rainfall variability and Indian Ocean sea surface temperature anomalies. *Earth Climate: The Ocean-Atmospheric interaction*, C. Wang, S.-P. Xie, and J. A. Carton, Eds., American Geophysical Union, Geophysical Monograph 147, Washington D. C., 325–345.

Wang, B., R. Wu, and X. Fu, 2000: Pacific-East Asia teleconnection: How does ENSO affect East Asian climate? *J. Climate*, **13**, 1517–1536.

Wang, B., B.-Q. Xiang, and J.-Y. Lee, 2013: Subtropical High predictability establishes a promising way for monsoon and tropical storm predictions. *Proceedings of the National Academy of Sciences of the United States of America*, **110**, 2718–2722.

Wang, Q., S.-L. Li, J.-J. Fu, and G.-P. Li, 2012: Formation of the anomalous summer precipitation in East China in 2010 and 1998: A comparison of the impacts of two kinds of El Niño. *Acta Meteorologica Sinica*, **26**, 665–682.

Wang, Y.-W., P.-M. Zhai, and H. Tian, 2006: Extreme high temperatures in southern China in 2003 under the background of climate change. *Meteorological Monthly*, **32**, 27–33. (in Chinese)

Wei, J., and J.-H. Sun, 2007: The analysis of summer heat wave and sultry weather in North China. *Climatic and Environmental Research*, **12**, 453–463. (in Chinese)

Wei, J., H. Yang, and S.-Q. Sun, 2004: Relationship between the anomaly longitudinal position of subtropical high in the western Pacific and severe hot weather in North China in summer. *Acta Meteorologica Sinica*, **62**, 308–316. (in Chinese)

Wu, B. Y., R. H. Zhang, B. Wang, and R. D'Arrigo, 2009: On the association between spring Arctic sea ice concentration and Chinese summer rainfall. *Geophys. Res. Lett.*, **36**, L09501, doi: 10.1029/2009GL037299.

Wu, R. G., 2002: A mid-latitude Asian circulation anomaly pattern in boreal summer and its connection with the Indian and East Asian summer monsoons. *Inter. J. Climatol.*, **22**, 1879–1895.

Wu, R. G., Z.-Z. Hu, and B. P. Kirtman, 2003: Evolution of ENSO-related rainfall anomalies in East Asia. *J. Climate*, **16**, 3742–3758.

Wu, R. G., and B. P. Kirtman, 2007: Observed relationship of spring and summer East Asian rainfall with winter and spring Eurasian snow. *J. Climate*, **20**, 1285–1304.

Xie, P. P., and P. A. Arkin, 1997: A 17-year monthly analysis based on gauge observations, satellite estimates, and numerical model outputs. *Bull. Amer. Meteor. Soc.*, **78**, 2539–2558.

Xie, S.-P., K.-M. Hu, J. Hafner, H. Tokinaga, Y. Du, G. Huang, and T. Sampe, 2009: Indian Ocean capacitor effect on Indo-western Pacific climate during the summer following El Niño. *J. Climate*, **22**, 730–747.

Yang, S., and K. M. Lau, 1998: Influences of sea surface temperature and ground wetness on Asian summer monsoon. *J. Climate*, **11**, 3230–3246.

Yasutomi, N., A. Hamada, and A. Yatagai, 2011: Development of a long-term daily gridded temperature dataset and its application to rain/snow discrimination of daily precipitation. *Global Environmental Research*, **15**, 165–172.

Ye, D.-X., J.-F. Yin, Z.-H., Chen, Y.-F. Zheng, and R.-J. Wu, 2013: Spatiotemporal change characteristics of summer heatwaves in China in 1961–2010. *Advances in Climate Change Research*, **9**, 15–20. (in Chinese)

Zou, X.-K., and H. Gao, 2007: Analysis of severe drought and heat wave over the Sichuan Basin in the Summer of 2006. *Advances in Climate Change Research*, **3**, 149–153. (in Chinese)